(Received 14 September 2023, Accepted 4 January 2024, Scheduled 4 February 2024)

Synthesis and Characterization of Polymer (PDMS-Fe_3O_4) Magneto-Dielectric Material Based on Complementary Double Split Ring Resonator

Fatin H. Ikhsan[1,*], Yee S. Khee[1], Samsul H. Dahlan[1], Fahmiruddin Esa[2], and Vahid Nayyeri[3]

[1] *Research Center for Applied Electromagnetic (EMCenter), Faculty of Electrical and Electronic Engineering Universiti Tun Hussein Onn Malaysia, Batu Pahat 86400, Malaysia*
[2] *Ceramic and Amorphous Group (CerAm), Faculty of Applied Sciences and Technology Pagoh Higher Education Hub, Universiti Tun Hussein Onn Malaysia, Panchor, Johor 84600, Malaysia*
[3] *School of Advanced Technologies, Iran University of Science and Technology, Tehran, Iran*

ABSTRACT: In this paper, a comparison microwave method between Transmission and Reflection using a Coaxial Cable and complimentary double split ring resonator (CDSRR) for characterization of magneto-dielectric material is proposed. This method enables the determination of both relative permittivity and permeability of magneto-dielectric material. The CDSRR resonates at 3.46 GHz with a quality factor of 127 in unloaded condition. To determine the effects of permittivity and permeability on the shift of resonant frequency, the electric and magnetic fields are localized in two separate zones in the CDSRR sensor. Prediction formulas are proposed to extract the value of real permittivity and permeability from S_{21} parameter. For Transmission/Reflection Method, to extract the dielectric and magnetic properties, Nicolson-Ross-Weir (NRW) are used. The prototypes of proposed sensors are fabricated on a ROGERS 3003 and tested for validation of their functionality. A good agreement between the measured data using Transmission/Reflection Method and CDSRR sensor is observed.

1. INTRODUCTION

Magneto-dielectric material has received considerable attention as it has wide range of application, for example, antenna miniaturization [1–4], radar absorbing materials [5, 6], electromagnetic interference (EMI) shielding [7], and wireless communication [8]. It is a type of composite material that demonstrates both magnetic and dielectric properties. Permittivity and permeability are indeed closely related to the characteristics of a material and are fundamental in representing the electromagnetic properties of a material. They are established based on the combination of magnetic and dielectric materials to enhance their individual properties [9]. Usually, both dielectric and magnetic materials have values greater than unity. This is because in antenna design, the antenna characteristic such as resonance [10], dimensions [11], antenna impedance [12], radiation pattern [13], and bandwidth [14] are sensitive to the variation of dielectric properties. Precisely, forming composite magneto-dielectric (MD) substrates with enhanced electromagnetic properties has been investigated using magnetic materials such as ferrites, nickel oxide, and iron oxide [2, 15].

Since then, the precise characterization of magneto-dielectric material is very crucial for efficient design and system performance prediction. Material characterization methods based on radio frequency (RF) and microwave measurements such as transmission/reflection method, free space method, and open-ended coaxial probe method have been extensively employed [16–18]. The method to be chosen is dependent on operating frequency, sample type, shape and size, the required accuracy and precision, non-destructive or destructive. Transmission/reflection method which is based on coaxial line and waveguide requires the material under test (MUT) to fit the cross section of the sample holder (coaxial line and waveguide) as the air gap introduces unwanted measurement inaccuracy that underestimates the actual dielectric properties of MUT [19, 20]. The free space dielectric measurement method suffers from diffraction and multiple reflection problems [19, 21]. Apart from this, the alignment between the transmitting, receiving antennas and the MUT must be taken care well to prevent any measurement imprecision. On the other hand, open-ended coaxial probe is suitable for liquid or semi-liquid materials that are as thick as the diameter of the probe [19, 21]. It is not suitable for solid material as the air gap between the probe and material surface gives rise to measurement discrepancies. This method is unable to characterize magnetic material too.

Lately, sensors based on microwave such as split-ring resonators (SRRs) and complementary split-ring resonators (CSRRs) are favorable too due to their low cost, high sensitivity, ease in sample preparation, and they can be fabricated affordably using printed circuit board etching technology [22–25].

This work utilizes a microstrip line-based resonator for the characterization of isotropic and homogenous materials. A

* Corresponding author: Fatin Hamimah Ikhsan (fatenikhsan@yahoo.com).

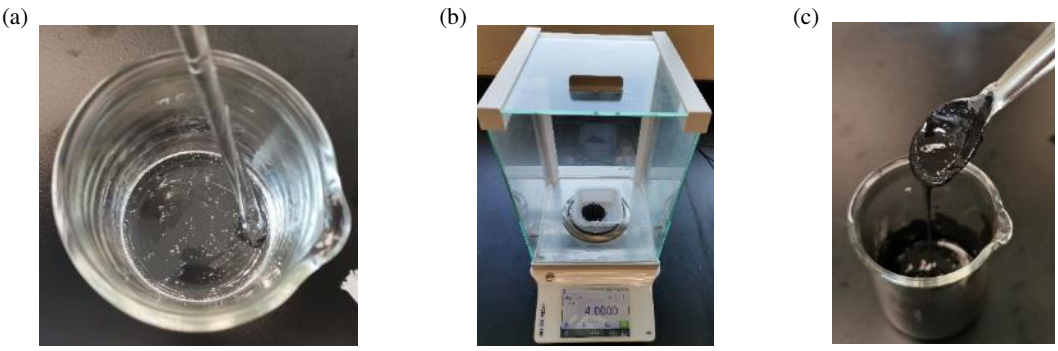

FIGURE 1. (a) PDMS. (b) Fe_3O_4 powder. (c) Mixture of PDMS-Fe_3O_4.

complementary double split-ring resonator (CDSRR) is presented as a microwave sensor to define the dielectric properties of a flexible magneto-dielectric material based on iron oxide (Fe_3O_4) and polydimethylsiloxane (PDMS). The CDSRR operates on the principle that induces high intensity of magnetic and electric fields at the sensing area, which is sensitive to variations of dielectric properties. For the ease of sample preparation, a cuboid type sample with size of $5\,\text{mm} \times 5\,\text{mm} \times 12\,\text{mm}$ requires a big sample which is considered demanding and expensive especially for magneto-dielectric material. For the purpose of validation, the measured dielectric properties will be confirmed with the reading from transmission/reflection method by using a APC-7 coaxial connector.

Overall, the paper is organized by firstly, explanation of synthesis process of PDMS-Fe_3O_4. The procedure of CDSRR design based on simulation CST Microwave Studio is described. It is then followed by experimental measurement procedure of the real relative permittivity and permeability of PDMS-Fe_3O_4 by using the CDSRR, and the comparison dielectric results are tabulated and discussed at the end of the paper.

2. METHODOLOGY

2.1. Synthesis of Polydimethylsiloxane-Fe_3O_4 (PDMS-Fe_3O_4)

In this work, the polymer of polydimethylsiloxane (PDMS) is integrated with magnetic iron oxide (Fe_3O_4) to form a magneto-dielectric material. PDMS is a silicon-based elastomer with good electrical and mechanical properties such as modified dielectric properties, isotropic and homogenous, flexibility, durability, and transparency [1, 2, 26–28]. The polymer PDMS, commercially known as Sylgard184 silicone elastomer, consists of two components which are the elastomer base and curing agent. The microparticles of (Fe_3O_4) in powder formulation is manufactured by Alfa Aesar. Fe_3O_4 is selected because of ease of controlling the magnetic properties, good dispersion, and dissolution characteristic during composition process with polymeric matrices [1, 2]. Figures 1(a)–(c) show the PDMS, Fe_3O_4, and their mixture.

The nanoparticles of Fe_3O_4 and polymer PDMS are synthesized using composition process. To produce the PDMS polymer, the elastomer base and curing agent are combined in a 10:1 ratio during the mixing process. This solution was then stirred with a glass rod until uniformly dispersed. The Fe_3O_4 nanoparticles are dispersed in PDMS with weight ratios $2:10$, $3:10$, $4:10$, $7:10$, and $10:10$. The PDMS and Fe_3O_4 are stirred well to ensure that the materials are homogenous. It is important to be noted that controlling the composition of Fe_3O_4 in the weight ratio is used to prevent the mixture from agglomerating during the stirred process. After the mixture was homogenous, it was placed in a vacuum desiccator for 25 minutes to remove bubbles. Finally, the mixture was poured into a toroidal mold and placed in room temperature for 24 hours. Figure 2 shows the fabricated sample in toroidal shapes.

FIGURE 2. Fabricated sample with different composition ratio of PDMS-Fe_3O_4.

2.2. Sensor Design

In this work, a complimentary double split ring resonator (CDSRR) is proposed for magneto dielectric material characterization. Generally, a simple resonator can be represented by an RLC circuit where its resonant frequency is given by (1)

$$f_{rn} = \frac{1}{2\pi\sqrt{LC}} \tag{1}$$

where L and C are the equivalent inductance and capacitance of the resonator. In accordance with perturbation theory, when a material under test (MUT) was placed on the electric and magnetic area of sensor, the sample will disturb the field distribution and cause the changes in resonant frequency and quality factor of resonator. The relation between the shifted resonant frequency and material properties of the MUT can be expressed

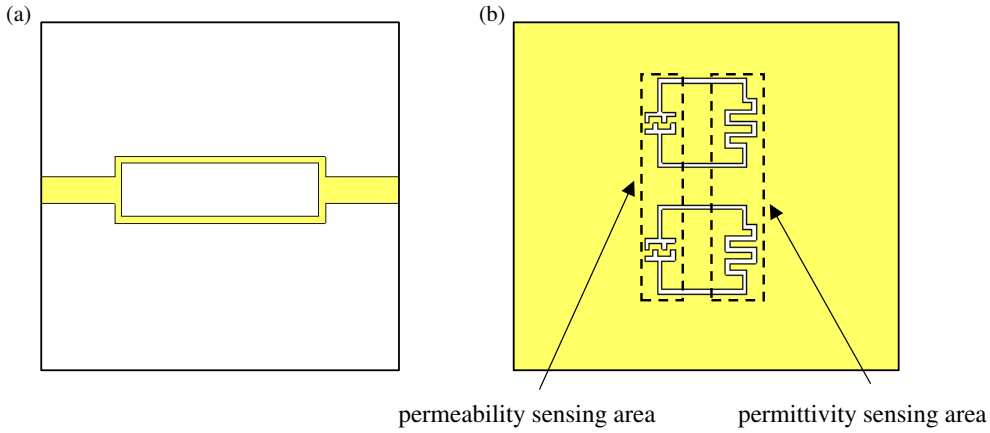

FIGURE 3. (a) Top side of CDSRR. (b) Bottom side of CDSRR.

FIGURE 4. A pair of APC7 connectors is used for dielectric measurement.

FIGURE 5. A pair of APC7 connectors with the sample.

as (2)

$$\frac{\Delta f_r}{f_{r\_\text{unloaded}}} = \frac{\int\limits_v^0 \Delta\varepsilon E_1 E_0 + \Delta\mu H_1 H_0 \mathrm{d}v}{\int\limits_v^0 \Delta\varepsilon_0 \left|E_0\right|^2 + \mu_0 \left|H_0\right|^2 \mathrm{d}v} \tag{2}$$

where f_{r_unloaded} is the resonance frequency for unloaded resonator, Δf_r the shifted resonant frequency when resonator loaded with MUT, ε_0 the free space permittivity, μ_0 the free space permeability, $\Delta\varepsilon = \varepsilon_0(\varepsilon_r - 1)$ the change in permittivity, and $\Delta\mu = \mu_0(\mu_r - 1)$ the change in permeability. E_0 and H_0 are the electric and magnetic fields without loading MUT; E_1 and H_1 are the disturbed fields; and v is the perturbed volume. In the resonator, if the electric field has a much higher intensity than the magnetic field, the change in magnetic permeability does not reflected significantly on the resonant frequency, but the permittivity can change the resonance frequency considerably. Thus, by loading MUT at high intensity electric field, changes in resonance frequency can indicate the sample/s permittivity, without regard to permeability of the sample. This is applied to the area with high intensity magnetic field too. For the purpose to achieve such "two single-field localized" regions for measurement, a CDSRR-based sensor is designed as shown in Figure 3.

2.3. Dielectric Measurement of PDMS-Fe_3O_4

Several methods for extracting the dielectric and magnetic properties of materials at microwave frequencies have been studied. This method can be categorized as non-resonant (transmission/reflection method) and resonant method (cavity perturbation technique) [16, 20, 24, 29, 30]. This work presents two material characterization methods, namely transmission/reflection methods (APC-7 coaxial connector) and microwave sensors based on CDSRRs, to obtain the relative permittivity (ε_r) and relative permeability (μ_r) of the magneto dielectric material. In transmission/reflection method, the dielectric and magnetic properties of material under test (MUT) are found by converting the transmission coefficient (S_{21}/S_{12}) and reflection coefficient (S_{11}/S_{22}) using Nicolson-Ross-Weir (NRW) conversion formulation. For CDSRRs, both the dielectric and magnetic properties of MUT are predicted based on resonance frequency shifting.

2.3.1. Transmission/Reflection Method Based on APC-7 Connectors

Dielectric measurement based on transmission/reflection method requires a pair of APC-7 connectors as shown in Figure 4 for dielectric and magnetic measurement in this work. The annular sample was placed into the slot as shown in Figure 5. Then, the two APC-7 connectors were combined and connected to the vector network analyzer (VNA) for S-parameter measurement between 1 GHz and 4 GHz, as

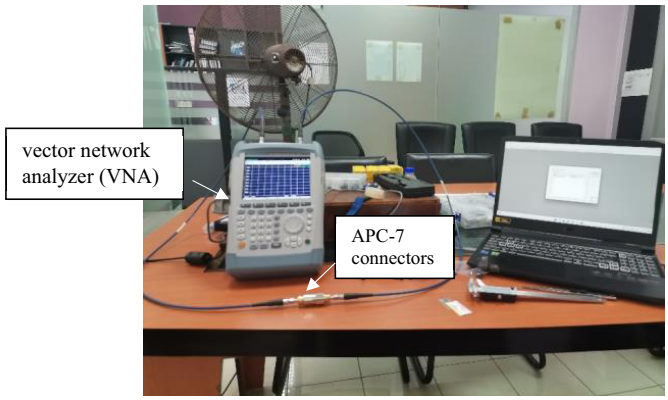

FIGURE 6. Dielectric measurement setup.

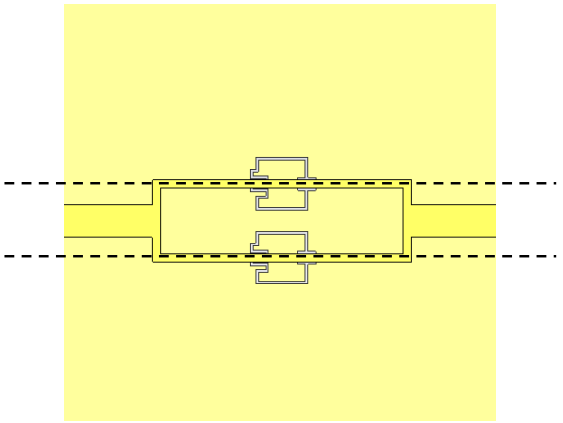

FIGURE 7. CDSRR with cross polarization excitation. The dashed lines show the magnetic wall of the loaded CSRR.

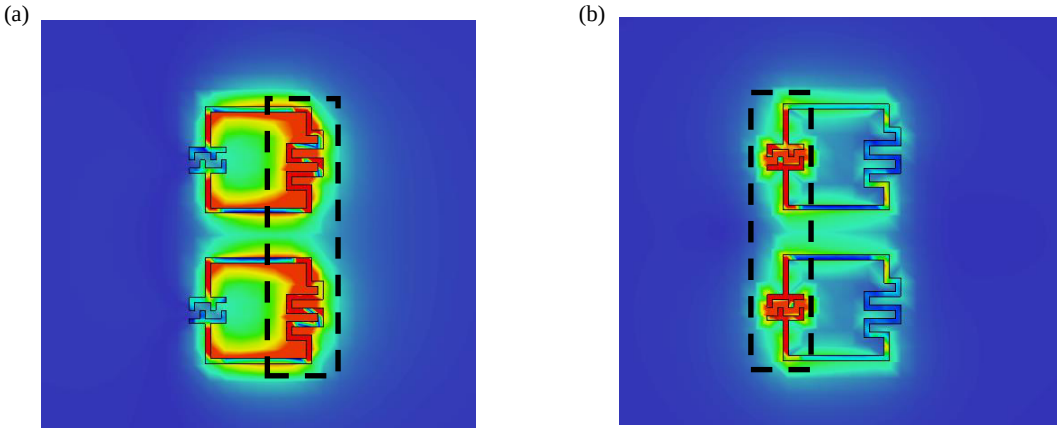

FIGURE 8. Proposed CDSRR sensor. (a) Electric field distribution. (b) Magnetic field distribution.

shown in Figure 6. The calibration process is carried out to ensure the accuracy and reliability of the measurement results. Nicolson-Ross-Weir conversion formulation [31] was used to extract the S-parameter to the dielectric and magnetic properties (relative permittivity and relative permeability) of PDMS-Fe_3O_4.

2.3.2. Microwave Sensor Based on CDSRR

In this paper, a Rogers RO3003 with a dielectric constant 3, a loss tangent of 0.001, and a thickness of 1.52 mm was used as a substrate of the microwave sensor. The width of the microstrip line at the top side is set to 3.781 mm to provide a characteristic impedance 50 Ω. In this paper, to enhance the sensitivity of sensor, a splitter-combiner microstrip section is used for the proper excitation of CDSRR. Two transmission lines were used to excite each resonator individually. CDSRR is etched on the metal ground plane. The CDSRR was designed and simulated by using CST Microwave Studio Suite. It is excited with maximum electric/magnetic excitation also called as cross polarization. This is because the magnetic wall of loaded CDSRR is parallel to the transmission line conducting strip as shown in Figure 7.

Figure 8 shows the CDSRR etched on the ground plane of the microstrip lines. The resonance frequency of CDSRR for simulation is 3.446 GHz with a Q-factor of 127 at unloaded condition. At the resonance frequency, the electric field, **E**, and magnetic field, **H**, distributions are depicted at Figures 8(a) and (b), respectively. At permittivity sensing area, **E** is localized with maximum intensity, and **H** is negligible. On the other hand, at region indicated as permeability sensing area, **H** is very high intensity, and **E** is near zero. These two zones are the most suitable locations for the magneto-dielectric material sample.

3. RESULT AND DISCUSSION

Figure 9 shows the extracted relative permittivity (ε_r) and relative permeability (μ_r) for five different ratios of PDMS-Fe_3O_4. In Figure 9(a), it is found that the extracted relative permittivity (ε_r) rises in all frequency range when the ratio of Fe_3O_4 increases. At 3.5 GHz, the $2:10$ PDMS-Fe_3O_4 has ε_r of 3.2 and increases to 4.79 at the ratio 10.10 of PDMS-Fe_3O_4, whereas the average ε_r is 3.4, 3.8, and 4.6 for $3:10, 4:10$ and $7:10$ of PDMS-Fe_3O_4, respectively. Figure 9(b) shows the extracted relative permeability (μ_r) for the five samples. Ratio $10:10$ has the highest value while ratio $2:10$ has the lowest value in between 1 GHz and 4 GHz. Drawing from observation, it is in-

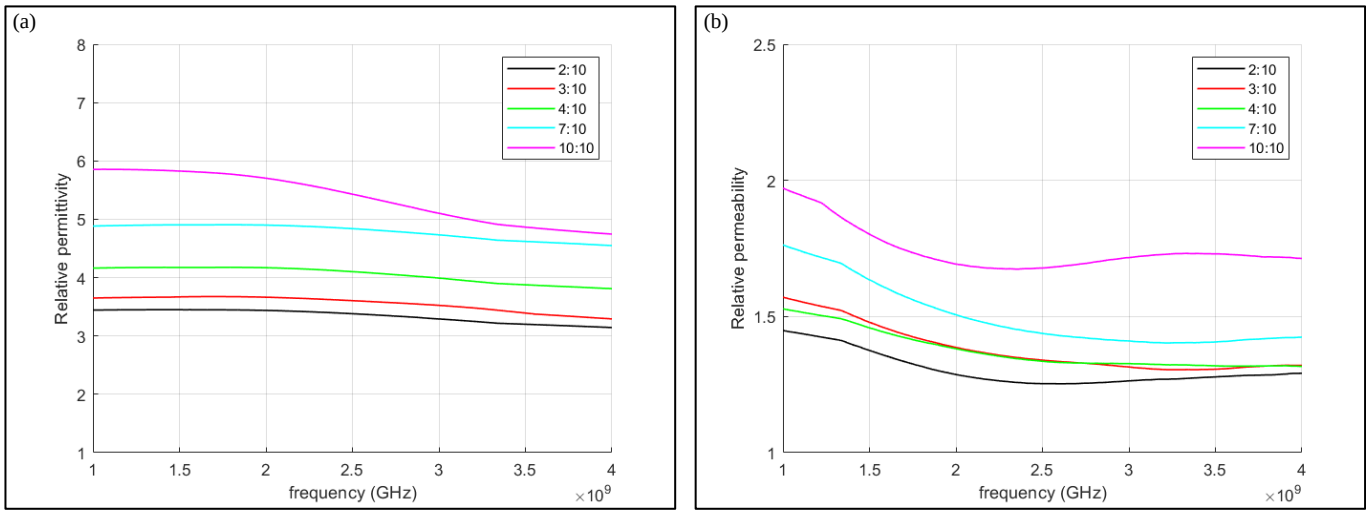

FIGURE 9. Frequency dependence of (a) relative permittivity, (b) relative permeability of PDMS-Fe_3O_4.

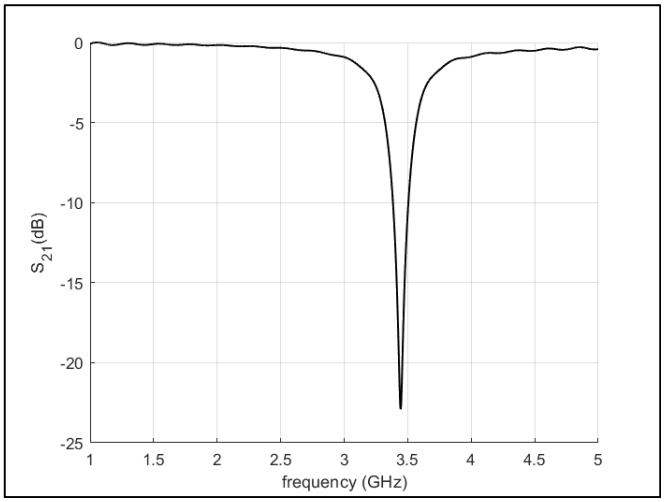

FIGURE 10. Magnitude of S_{21} for empty CDSRR.

teresting to notice that ratios $3:10$ and $4:10$ produce similar relative permeability in between 1 GHz and 4 GHz. The investigation shows that as the ratio of Fe_3O_4 increases, μ_r increase from 1.28 ($2:10$) to 1.75 ($10:10$) at 3.5 GHz. For other samples, $3:10, 4:10$ and $7:10$, μ_r is 1.3, 1.31, and 1.4, respectively.

Based on the simulation, the resonance frequency of the sensor in unloaded condition occurs at 3.446 GHz with the quality factor of 127 as shown in Figure 10. With the goal of forming prediction formulation for material characterization, the sensor is loaded with MUTs having different relative permittivity ($\varepsilon_r = 1$–10) and relative permeability ($\mu_r = 1$–3). Both the electric and magnetic loss tangent ($\tan\delta_m$ and $\tan\delta_e = 0$) are set as 0 in the simulation. When the MUTs are loaded at the sensing areas, they change the field distribution and capacitance in (1) and hence result in different loaded resonance frequencies and quality factors. In this work, the MUT thickness is fixed to 5 mm. This thickness is chosen as continuously increasing the sample thickness would not introduce changes in resonance frequency and quality factor. 50 µm of air gap is introduced between MUT and the sensing area in the simulation to consider the air gap due to surface roughness of the MUT.

When the MUT was placed at the permeability sensing area for different values of μ_r, $\tan\delta_m = 0$, the resonance frequency of the CDSRR is shifted to the lower values as shown in Figure 11(a). At this permeability sensing area, E field distribution is low, and the variation of ε_r does not affect the resonance frequency shifting and quality factor. Thus, the change of resonance frequency is due to the variation of relative permeability of MUT. It is indicated that when μ_r is increased from 1 to 3, the resonance frequency decreases from 3.446 GHz to 3.12 GHz. Figure 11(b) shows the relative permeability as a function of normalized resonance frequency by using curve fitting technique, and it can be represented a third order polynomial function in (3)

$$\mu_r = 339.7(f_{rn}^3) - 965.7(f_{rn}^2) + 922.4(f_{rn}) - 295.5 \quad (3)$$

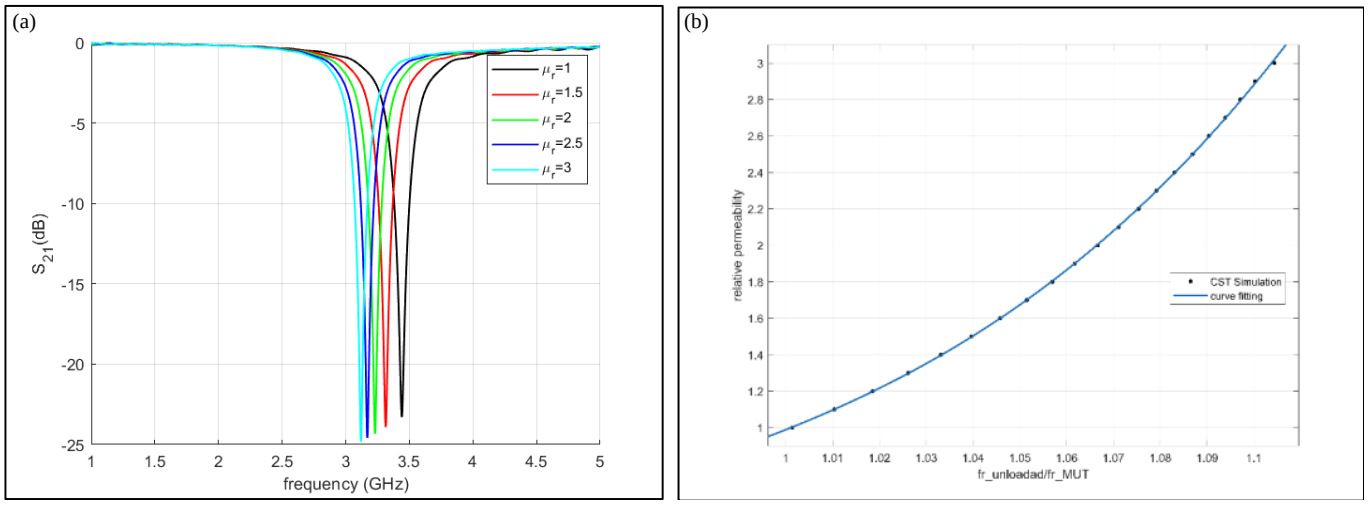

FIGURE 11. (a) Sensor response for different μ_r when $\tan\delta_m = 0$. (b) The real part of the permittivity μ_r of the MUT function of the normalized resonance frequency.

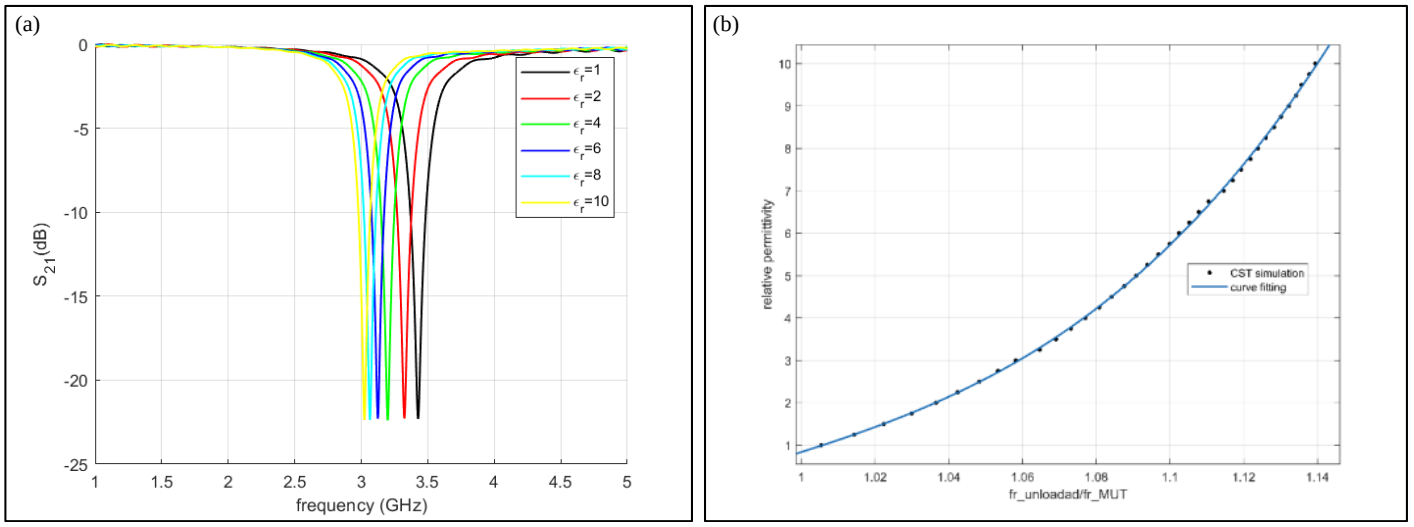

FIGURE 12. (a) Sensor response for different ε_r when $\tan\delta_e = 0$. (b) The real part of the permittivity ε_r of the MUT function of the normalized resonance frequency.

where f_{rn} is the normalized resonance frequency, f_{r_unloaded} the response frequency without MUT, and $f_{r\text{MUT}}$ the resonance frequency when MUT is placed at the sensing area.

$$f_{rn} = \frac{f_{r\_\text{unloaded}}}{f_{r\text{MUT}}} \tag{4}$$

Figure 12(a) shows the response for different values of ε_r when $\tan\delta_e = 0$. Obviously, by increasing ε_r from 1 to 10, the resonance frequency decreases from 3.446 GHz to 2.4 GHz. In this permittivity sensing area, **H** field distribution is low, hence the resonance frequency is a function of only ε_r. Figure 12(b) shows the relative permittivity of MUT as a function of normalized resonance frequency. By using curve fitting tool, a second order polynomial function was proposed for extracting the relative permittivity in terms of normalized resonance frequency as (5)

$$\varepsilon_r' = 397.6(f_{rn}^2) - 788.5(f_{rn}) - 392 \tag{5}$$

The CDSRR sensor was fabricated as shown in Figures 13(a) and (b). It is excited with two SMA connectors and connected to a vector network analyzer. The measured unloaded resonance frequency and quality factor of fabricated CDSRR are 3.46 GHz and 123, respectively, which are in a good agreement with the simulated results as shown in Figure 14(a). The magneto-dielectric material with sample size 5 mm × 5 mm × 12 mm was prepared to fit in both of the sensing areas. Hence, only a sample is required to measure both relative permittivity and relative permeability. The permittivity and permeability sensing areas were loaded with different ratios of PDMS-Fe_3O_4.

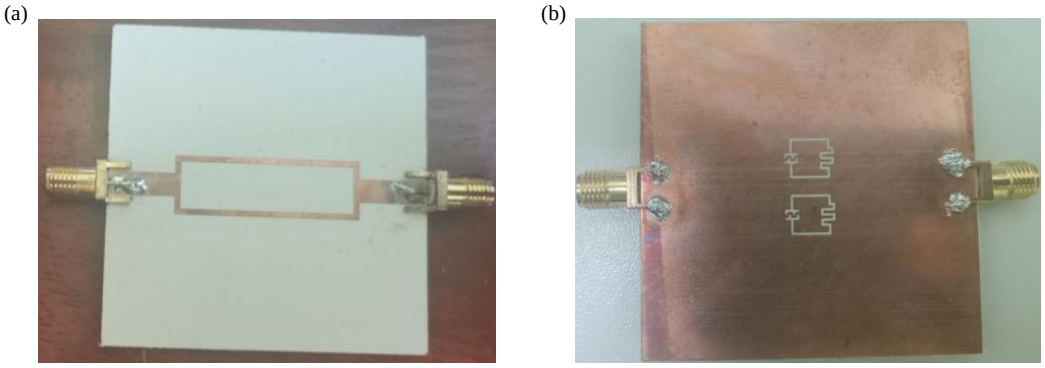

FIGURE 13. (a) Top view and (b) bottom view of proposed sensor.

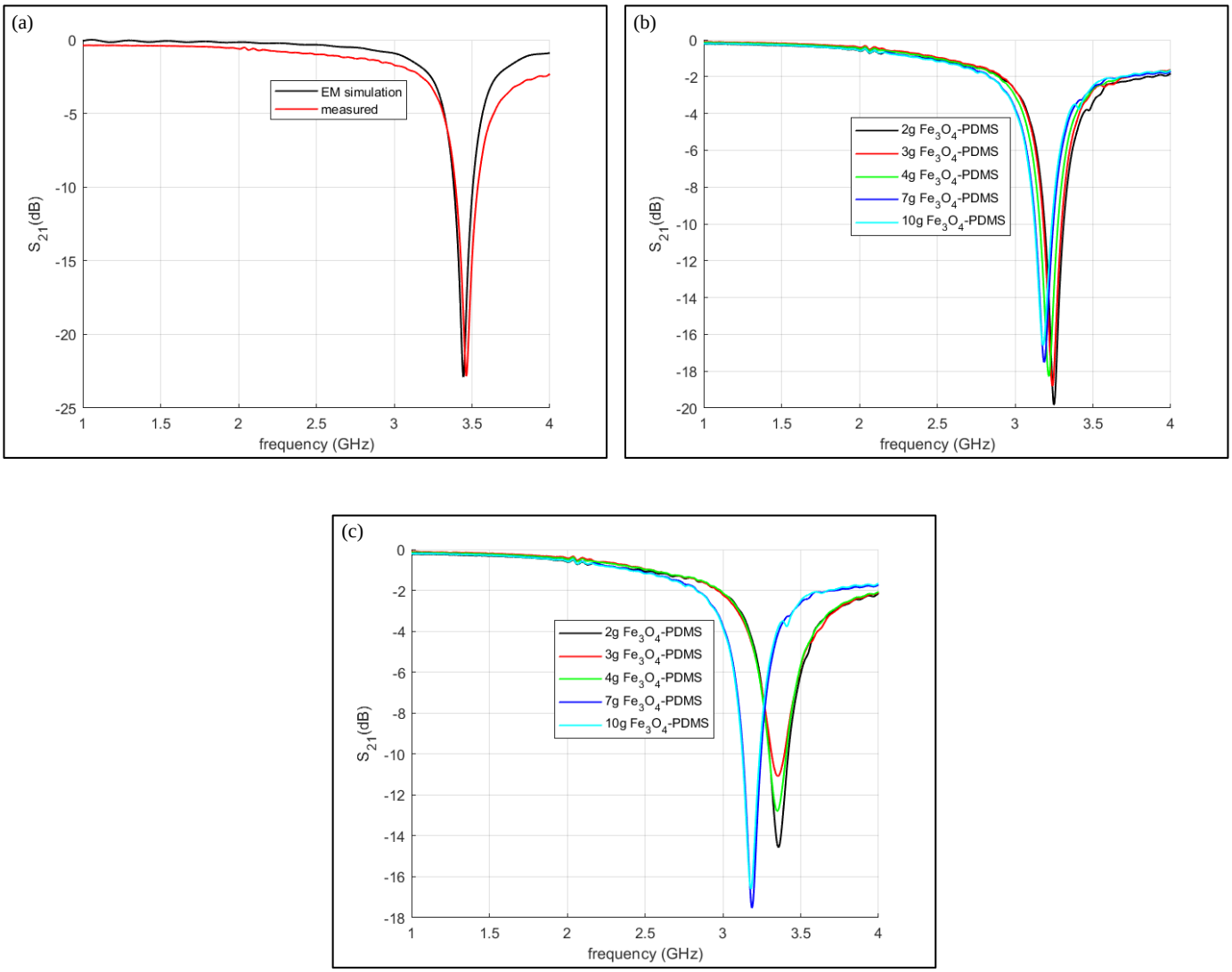

FIGURE 14. (a) Comparison between the simulated and measured S_{21} of the unloaded sensor, (b) measured S_{21} of the sensor when different samples are loaded in permittivity sensing area and (c) permeability sensing area.

Based on the measured S_{21} as shown in Figures 14(b) and (c), the resonance frequencies are applied in (3)–(5) for the calculation of relative permittivity, ε_r, and relative permeability, μ_r. The measured values obtained from transmission/reflection method and microwave sensor are compared in Table 1. The results are in good agreement.

TABLE 1. Measured dielectric and magnetic of different ratio of PDMS-Fe_3O_4.

MUT	ε_r		μ_r	
	CDSRR	Transmission/Reflection Method	CDSRR	Transmission/Reflection Method
2 gram	3.230	3.210	1.283	1.282
3 gram	3.390	3.4	1.3	1.3
4 gram	3.863	3.866	1.31	1.31
7 gram	4.616	4.615	1.41	1.4
10 gram	4.770	4.790	1.745	1.747

4. CONCLUSION

This work has presented the synthesis and characterization of PDMS-Fe_3O_4 by using resonator method (CDSRR). The CDSRR has been designed and fabricated, and testing has been conducted on PDMS-Fe_3O_4 to characterize their dielectric properties at 3.5 GHz. The empirical models of the proposed sensors, which were derived through the utilization of numerical methods and curve fitting techniques, have been subjected to experimental verification. The measured relative permittivity and relative permeability values exhibit a significant degree of conformity with the values found from transmission/reflection technique based on APC-7 coaxial connector.

ACKNOWLEDGEMENT

Communication of this research is made possible through monetary assistance by Universiti Tun Hussein Onn Malaysia and the UTHM Publisher's Office via Publication Fund E15216.

REFERENCES

[1] Adhiyoga, Y. G., S. F. Rahman, C. Apriono, and E. T. Rahardjo, "Magneto-dielectric properties of PDMS-magnetite composite as a candidate for compact microstrip antennas in the C-band 5G frequency," *Journal of Materials Science-Materials in Electronics*, Vol. 32, No. 8, 11 312–11 325, Apr. 2021.

[2] Alqadami, A. S. M., B. Mohammed, K. S. Bialkowski, and A. Abbosh, "Fabrication and characterization of flexible polymer iron oxide composite substrate for the imaging antennas of wearable head imaging systems," *IEEE Antennas and Wireless Propagation Letters*, Vol. 17, No. 8, 1364–1368, Aug. 2018.

[3] Muhamad, W. A. W., R. Ngah, M. F. Jamlos, P. J. Soh, M. T. Ali, and A. Narbudowicz, "Bandwidth enhancement of a multilayered polymeric comb array antenna for millimeter-wave applications," *Applied Physics A-Materials Science & Processing*, Vol. 123, No. 1, 1–4, Jan. 2017.

[4] Zheng, Z., "Performance based on magneto-dielectric ferrite materials," *IEEE Transactions on Magnetics*, Vol. 56, No. 3, 5, 2020.

[5] Yadav, R. and R. Panwar, "Structure for stealth applications," *IEEE Transactions on Magnetics*, Vol. 58, No. 1, 1–5, 2022.

[6] Panwar, R. and J. R. Lee, "Performance and non-destructive evaluation methods of airborne radome and stealth structures," *Measurement Science and Technology*, Vol. 29, No. 6, Jun. 2018.

[7] Qian, K., Q. Li, A. Sokolov, C. Yu, P. Kulik, O. Fitchorova, Y. Chen, C. Chinnasamy, and V. G. Harris, "Electromagnetic shielding effectiveness of amorphous metallic spheroidal- and flake-based magnetodielectric composites," *Journal of Materials Science & Technology*, Vol. 83, 256–263, 2021.

[8] Zheng, Z., Q. Feng, and Q. Xiang, "Low-loss NiZnCo ferrite processed at low sintering temperature with matching permeability and permittivity for miniaturization of VHF-UHF antennas," *Journal of Applied Physics*, Vol. 121, 063 901(1–7), 2017.

[9] Yao, X., J.-P. Zhou, X.-L. Zhang, and X.-M. Chen, "Magnetodielectric mechanism and application of magnetoelectric composites," *Journal of Magnetism and Magnetic Materials*, Vol. 550, 169099, Jan. 2022.

[10] Schaubert, D. H., D. M. Pozar, and A. Adrian, "Effect of microstrip antenna substrate thickness and permittivity: Comparison of theories with experiment," *IEEE Transactions on Antennas and Propagation*, Vol. 37, No. 6, 677–682, 1989.

[11] Pozar, D. M., *Microwave Engineering*, John Wiley & Sons, 2011.

[12] Kim, J. H. and J. Bang, "Antenna impedance matching using deep learning," *Sensors*, Vol. 21, No. 20, 1–10, Oct. 2021.

[13] Li, W., J. Ren, B. Zhang, Y.-T. Liu, H. Zhang, Y. Yin, and M. Shen, "Wideband dielectric patch antenna with stable radiation pattern," *IEEE Antennas and Wireless Propagation Letters*, Vol. 22, No. 7, 1716–1720, Jul. 2023.

[14] Calisir, I., X. Yang, E. L. Bennett, J. Xiao, and Y. Huang, "Enhancing the bandwidth of antennas using polymer composites with high dielectric relaxation," *Materials Today Electronics*, Vol. 3, 100026, Feb. 2023.

[15] Mosallaei, H. and K. Sarabandi, "Magneto-dielectrics in electromagnetics: Concept and applications," *IEEE Transactions on Antennas and Propagation*, Vol. 52, No. 6, 1558–1567, Jun. 2004.

[16] Costa, F., M. Borgese, M. Degiorgi, and A. Monorchio, "Electromagnetic characterisation of materials by using transmission/reflection (T/R) devices," *Electronics*, Vol. 6, No. 4, Dec. 2017.

[17] Hakansson, E., A. Amiet, and A. Kaynak, "Dielectric characterization of conducting textiles using free space transmission measurements: Accuracy and methods for improvement," *Synthetic Metals*, Vol. 157, No. 24, 1054–1063, Dec. 2007.

[18] Maenhout, G., T. Markovic, I. Ocket, and B. Nauwelaers, "Effect of open-ended coaxial probe-to-tissue contact pressure on dielectric measurements," *Sensors*, Vol. 20, No. 7, 1–13, Apr. 2020.

[19] Khan, M. T. and S. M. Ali, "A brief review of measuring techniques for characterization of dielectric materials," *International Journal of Information Technology and Electrical Engineering*, Vol. 1, No. 1, 1–5, 2012.

[20] Dubrovskiy, S. and K. Gareev, "Measurement method for detecting magnetic and dielectric properties of composite materials at microwave frequencies," in *Proceedings of the 2015 IEEE North West Russia Section Young Researchers in Electrical and Elec-*

tronic Engineering Conference (2015 ElConRusNW), 24–26, St. Petersburg, Russia, Feb. 2015.

[21] Venkatesh, M. S. and G. S. V. Raghavan, "An overview of dielectric properties measuring techniques," *Canadian Biosystems Engineering*, Vol. 47, No. 7, 15–30, 2005.

[22] Javed, A., A. Arif, M. Zubair, M. Q. Mehmood, and K. Riaz, "A low-cost multiple complementary split-ring resonator-based microwave sensor for contactless dielectric characterization of liquids," *IEEE Sensors Journal*, Vol. 20, No. 19, 11 326–11 334, 2020.

[23] Shafi, K. T. M., A. K. Jha, and M. J. Akhtar, "Improved planar resonant RF sensor for retrieval of permittivity and permeability of materials," *IEEE Sensors Journal*, Vol. 17, No. 17, 5479–5486, Sep. 2017.

[24] Zhao, W.-S., H.-Y. Gan, L. He, Q. Liu, W. Wang, K. Xu, S. Chen, L. Dong, and G. Wang, "Microwave planar sensors for fully characterizing magneto-dielectric materials," *IEEE Access*, Vol. 8, 41 985–41 999, 2020.

[25] Saadat-Safa, M., V. Nayyeri, M. Khanjarian, M. Soleimani, and O. M. Ramahi, "A CSRR-based sensor for full characterization of magneto-dielectric materials," *IEEE Transactions on Microwave Theory and Techniques*, Vol. 67, No. 2, 806–814, Feb. 2019.

[26] Alqadami, A. S. M., M. F. Jamlos, and M. A. Jamlos, "Efficacy of a wideband flexible antenna on a multilayer polymeric nanocomposites Fe_3O_4-PDMS substrate for wearable applications," *Current Applied Physics*, Vol. 19, No. 11, 1259–1265, 2019.

[27] Hamouda, Z., J.-L. Wojkiewicz, A. A. Pud, L. Kone, S. Bergheul, and T. Lasri, "Magnetodielectric nanocomposite polymer-based dual-band flexible antenna for wearable applications," *IEEE Transactions on Antennas and Propagation*, Vol. 66, No. 7, 3271–3277, 2018.

[28] Shueai, A., M. Alqadami, and M. Faizal, "Assessment of PDMS technology in a MIMO antenna array," *IEEE Antennas and Wireless Propagation Letters*, Vol. 15, 1939–1942, 2015.

[29] Maleki, M., S. H. M. Armaki, and E. Hamidi, "Study of ferrite material characterization using transmission line model," *Microwave and Optical Technology Letters*, Vol. 60, No. 12, 2876–2880, Dec. 2018.

[30] Shafi, M. K. T., A. K. Jha, and M. J. Akhtar, "Dual band RF sensor for testing of magnetic properties of materials using meandered line SRR," *Sensors and Actuators A-Physical*, Vol. 272, 170–177, Apr. 2018.

[31] Sahin, S., N. K. Nahar, and K. Sertel, "A simplified Nicolson-Ross-Weir method for material characterization using single-port measurements," *IEEE Transactions on Terahertz Science and Technology*, Vol. 10, No. 4, 404–410, Jul. 2020.